A New Type of Bunch Compressor and Seeding of a Short Wave Length Coherent Radiation[*]

A.A. Zholents

Advanced Photon Source, Argonne National Laboratory
Argonne, IL 60439

M.S. Zolotorev

Lawrence Berkeley National Laboratory,
Berkeley, CA, 94720

To be published as a Light Source Technical Notes

A New Type of Bunch Compressor and Seeding of a

Short Wave Length Coherent Radiation

A.A. Zholents[1] and M.S. Zolotorev[2]

[1]Argonne National Laboratory, Argonne, Illinois, 60439, USA

[2]Lawrence Berkeley National Laboratory, Berkeley, California, 94720, USA

ABSTRACT

Transverse-to-longitudinal emittance exchange was proposed in [1] as a tool for an effective matching of the electron beam phase space to requirements of a possible application. Here we propose a new purpose, namely, use of two consecutive emittance exchanges equipped with the telescope between them for a bunch compression that can be done without the energy chirp in the electron bunch. In principle it allows to reduce the electron peak current in the linac by moving the bunch compressor to the end of the linac and, thus, to relax collective effects associated with high peak currents. It is also possible to have a split-action compression when the first part is done inside the low-energy part of the linac and the second and final part is done after the linac. We also demonstrate how proposed bunch compressor can be used for frequency up-conversion of the energy modulation provided by the laser interacting with the electron beam and thus can prepare a significantly higher frequency seed for seeded free-electron lasers. The same approach can be used for a frequency down-conversion that can be useful for generation of THz radiation.

1. Introduction

Bunch compressors play an important role in the physics of charged particle beams. Many applications require high peak current beams, which are obtained by taking low peak current beams from the injector and compressing them after acceleration to relativistic energy. A widely used method of compression consists of creating a linear energy variation along the bunch of particles (chirp) using the off-crest acceleration in the rf linac and sending this bunch through a magnetic lattice with time-of-flight dispersion, often called a bunch compressor [2]. A compression is achieved by exploring the path length differences of particle trajectories with different energies.

In this paper we propose a new type of a bunch compressor that does not need an energy chirp. This proposal takes advantage of the emittance exchange transformation proposed in [1] and further developed and tested in [3, 4]. We consider doing compression in three principle steps. First, we exchange the longitudinal and horizontal emittances. Second, using the magnetic telescope we expand the horizontal beam size and squeeze its angular size. Finally, we reverse emittance exchange and return to the original horizontal and longitudinal emittances, but in a new state with compressed bunch length and increased energy spread.

In next section we describe this new scheme in detail. After that we analyze possible collective effects due to space charge forces that are applicable to all types of charged particle beams and due to coherent synchrotron radiation that are specific only to the electron beam. Finally we discuss several applications of the proposed scheme going beyond just bunch compression.

2. Bunch compression

Figure 1 shows a schematic of a proposed bunch compressor. It begins and ends with the emittance exchange lattice and has FODO optics in the middle that acts as the magnetic telescope. For illustration of our goal we adapt here the simplest emittance exchange lattice, although many more variants also exist (see, Appendix). Each emittance exchange lattice is composed of two $-I$ beam transport sections containing two bending magnets and a FODO lattice. A key element of the emittance exchange scheme is a radio frequency (rf) deflecting cavity operating in TM_{110} mode [1]. An electron energy gain in this cavity depends on an electron horizontal coordinate, and in a thin length approximation is equal to

$$\delta = \frac{2eV_0}{E} J_1(x/\lambdabar_{rf}) \cos(\omega_{rf} t) \approx \frac{eV_0}{E\lambdabar_{rf}} x = k\,x\,. \tag{1}$$

Here E is the equilibrium electron beam energy, $\delta = \Delta E/E$ is the relative energy deviation, J_1 is the Bessel function of the first kind, $\omega_{rf} = c/\lambdabar_{rf}$ is the frequency of the electromagnetic field oscillations in the cavity, $\lambdabar_{rf}$ is the reduced rf wavelength, c is the speed of light, e is the electron charge, V_0 is the cavity's total "transverse" voltage, and t is the time. It is assumed that the bunch center passes the cavity at $t = 0$. Particles passing the cavity at different times receive kicks in the horizontal direction due to the cavity's magnetic field

$$\Delta x' = \frac{2eV_0}{E} \frac{J_1(x/\lambdabar_{rf})}{x/\lambdabar_{rf}} \sin(\omega_{rf} t) \approx \frac{eV_0}{E\lambdabar_{rf}} ct \approx k\,z\,, \tag{2}$$

where z is the longitudinal position of the particle within the bunch with respect to the bunch center.
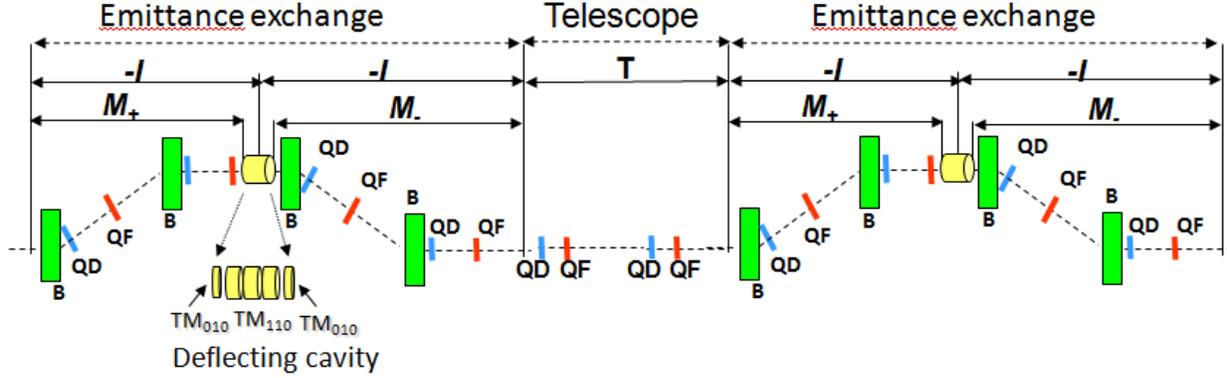
Figure 1. A schematic of the bunch compressor. Here B is bend magnet, and QD and QF are defocusing and focusing quadrupoles. The insert shows the deflecting cavity surrounded by ordinary accelerating cavities.

A multi-cell deflecting cavity of length d_1 affects particles in a slightly more cumbersome way described by a 4×4 transport matrix for a four-dimensional coordinate vector with components (x, x', z, δ), where x' is the angle. For simplicity, we ignore the vertical motion because no coupling to the vertical motion is produced in the bunch compressor to the first order of the beam transport and obtain [1]

$$TCAV = \begin{bmatrix} 1 & d_1 & kd_1/2 & 0 \\ 0 & 1 & k & 0 \\ 0 & 0 & 1 & 0 \\ k & kd_1/2 & k^2 d_1/6 & 1 \end{bmatrix}. \tag{3}$$

We note that the thick deflecting cavity also supplies energy gain that is quadratic with k due to a combined effect of the magnetic and electric fields, i.e., the magnetic field pushes particles aside and the electric field changes their energies while they gain horizontal offsets. This energy gain can be compensated by using the TM_{010} mode accelerating cavity next to the deflecting cavity or two such cavities with half strength, i.e., one on each side of the deflecting cavity as shown with the insert in Figure 1. We note that the phases of the rf fields in all three cavities should be strictly synchronized. Although the accelerating cavities can operate at a different frequency

than the frequency of the deflecting cavity, it is more convenient to use the same frequency. In this case the total accelerating voltage in each side cavity V_1 can be derived from the equation below, which ensures removal of the acceleration term in (3):

$$\frac{eV_1}{E} \approx -\frac{d_1}{12\lambda_{rf}}\left(\frac{eV_0}{E}\right)^2.$$

(4)

In this case a 4×4 transport matrix of a multi-cell side accelerating cavity of length $d_2/2$ in a linear approximation takes the form

$$C = \begin{bmatrix} 1 & d_2/2 & 0 & 0 \\ 0 & 1 & 0 & 0 \\ 0 & 0 & 1 & 0 \\ 0 & 0 & -k^2 d_1/12 & 1 \end{bmatrix},$$

(5)

and the entire transport through all three cavities takes the form

$$DEF = C \cdot TCAV \cdot C = \begin{bmatrix} 1 & d & kd/2 & 0 \\ 0 & 1 & k & 0 \\ 0 & 0 & 1 & 0 \\ k & kd/2 & 0 & 1 \end{bmatrix},$$

(6)

where $d = d_1 + d_2$ is the total length occupied by all three cavities. Therefore, the electron beam transport from the entrance of the emittance exchange lattice to the set of cavities located at a distance $d/2$ before the end of the first $-I$ transport as shown if Figure 1 is described by the matrix

$$M_+ = \begin{bmatrix} -1 & d/2 & 0 & \eta \\ 0 & -1 & 0 & 0 \\ 0 & -\eta & 1 & \xi \\ 0 & 0 & 0 & 1 \end{bmatrix},$$

(7)

where η is the dispersion function in the deflecting cavity and ξ is the time-of-flight parameter of this lattice section. Similarly, the beam transport from the end of the set of the cavities to the end of the emittance exchange lattice as shown if Figure 1 is described by the matrix

$$M_- = \begin{bmatrix} -1 & d/2 & 0 & -\eta \\ 0 & -1 & 0 & 0 \\ 0 & \eta & 1 & \xi \\ 0 & 0 & 0 & 1 \end{bmatrix} . \tag{8}$$

Finally, using $k\eta \equiv -1$ as suggested in [1], we obtain for the entire emittance exchange lattice:

$$EEX = M_- \cdot DEF \cdot M_+ = \begin{bmatrix} 0 & 0 & 0 & -\eta \\ 0 & 0 & -k & -k\xi \\ -k\xi & -\eta & 0 & 0 \\ -k & 0 & 0 & 0 \end{bmatrix} \tag{9}$$

After the first emittance exchange we have a new arrangement where the former longitudinal emittance and coordinates appear as the transverse emittance and coordinates and the former transverse emittance and coordinates appear as the longitudinal emittance and coordinates. This arrangement opens a broad range of opportunities to manipulate the former distribution of particles in the longitudinal phase space using known methods of beam manipulation in the transverse phase space. For example, here we demonstrate compression of the bunch. In order to do it we expand the transverse beam size and reduce its angular size using a magnetic telescope with the demagnification factor m described by the following transport matrix:

$$T = \begin{bmatrix} -m & 0 & 0 & 0 \\ 0 & -1/m & 0 & 0 \\ 0 & 0 & 1 & 0 \\ 0 & 0 & 0 & 1 \end{bmatrix} \tag{10}$$

6

Following the telescope in Figure 1 is the second emittance exchange lattice, which is exactly the same as the first one. It converts transverse coordinates to the longitudinal coordinates and *vice versa*, and, thus, returns back the former four-dimensional phase space, but with the modified structure of the longitudinal phase space as a result of the telescope's action, as seen from the product of all three transformations:

$$EEX \cdot T \cdot EEX = \begin{bmatrix} -1 & 0 & 0 & 0 \\ k^2\xi & -1 & 0 & 0 \\ 0 & 0 & \dfrac{1}{m} & \xi(\dfrac{1}{m}+m) \\ 0 & 0 & 0 & m \end{bmatrix}. \tag{11}$$

Besides bunch compression, the above transformation also produces the energy chirp $d\delta/dz = (\xi(1+1/m^2))^{-1}$ that can be obtained from (11). One can chose to remove this energy chirp right away or do it later. For example, deferred compression can be advantageous in many cases, allowing acceleration of an only partially compressed bunch with a smaller peak current and completing compression at the end of the linac before beam utilization. In this case the lattice section between the linac and the area of beam utilization should have a time-of-flight parameter $R_{56} = -\xi(1+1/m^2)E_2/E_1$, where E_2 is the final energy, and E_1 is the energy before acceleration. We also note that off-crest acceleration and longitudinal wakefields of the accelerating structure may modify the magnitude of the energy chirp, and it should be accounted for before deciding on the exact value of the R_{56} in this lattice section.

Finally, after removing the energy chirp we obtain:

$$BC = \begin{bmatrix} -1 & 0 & 0 & 0 \\ k^2\xi & -1 & 0 & 0 \\ 0 & 0 & \dfrac{1}{m} & 0 \\ 0 & 0 & 0 & m \end{bmatrix} \quad \text{and thus } \sigma_{z_f} = \frac{1}{|m|}\sigma_{z_i}, \quad \sigma_{\delta_f} = |m|\sigma_{\delta_i}, \qquad (12)$$

where $\sigma_{z_i}, \sigma_{z_f}$ and $\sigma_{\delta_i}, \sigma_{\delta_f}$ are initial and final rms bunch length and initial and final rms bunch energy spread, respectively. We note that adding –I transport before or after the telescope or using the telescope with all positive matrix elements will have a result similar to changing m to $-m$ in (12). Such a transformation creates the opportunity for a self compensation of the effects caused by the wakefields because it exchanges the locations of the particles inside the bunch, i.e., particles that were at the head of the bunch before compression will move to the tail of the bunch after compression and *vice versa*. Equation (12) also shows that cavities produce a weak focusing in the transverse plane with the equivalent focal length $f = 1/k^2\xi$.

Figure 2 shows the evolution of the particle distribution in the longitudinal and transverse phase space along the bunch compressor. In making this plot we designed the lattice of the bunch compressor following the above described recipe and chose an electron beam with the following parameters: beam energy of 350 MeV, normalized horizontal and vertical emittance of 0.8 mm-mrad, rms bunch length of 240 μm, rms relative energy spread of 10^{-4}, $\eta = 20$ cm, $\xi = -2$ cm, and Twiss functions at the entrance of the bunch compressor $\beta_x = 0.25$ m, and $\alpha_x = 0$. These parameters are considered to be representative, rather than fully optimized.
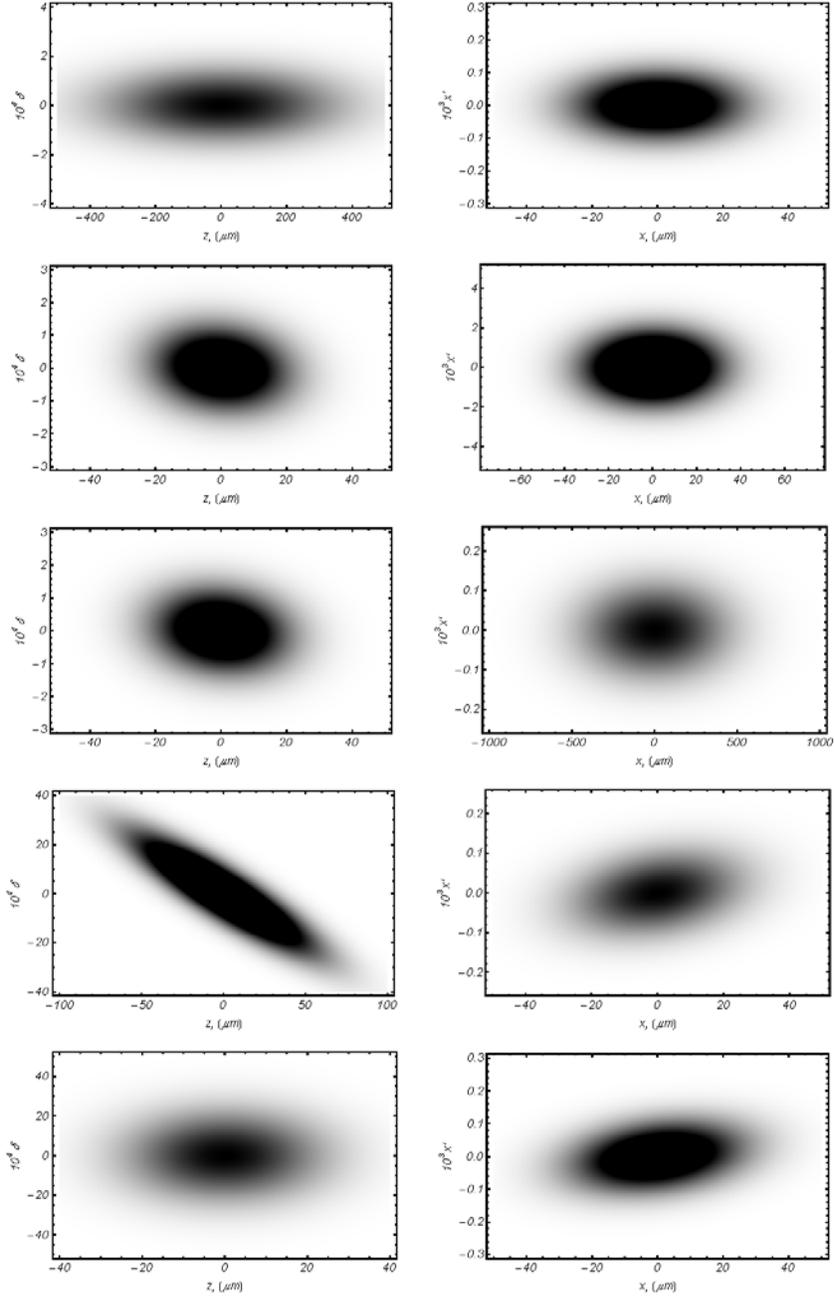
Figure 2. Density plots showing evolution of the particle distribution in the longitudinal (left column) and transverse (right column) phase space from top to bottom in order from location 1 to location 4 in Figure 1. The last row is a final distribution obtained after removal of the energy chirp.

3. Collective effects

First we consider emittance degradation triggered by the discreteness (shot noise) of particles in the bunch. We note that the first emittance exchange section converts particle density modulation along the x' coordinate at the entrance of the bunch compressor into the longitudinal density modulation in the telescope section. Then the longitudinal electric field induced by the space charge in the presence of this modulation creates energy modulation of particles while the bunch passes through the telescope section. Finally, the second emittance exchange section converts it into the transverse coordinate modulation. Thus, the entire bunch compressor amplifies particle density modulation in the transverse phase space.

In what follows, we estimate the emittance growth for a case when the shot noise of electrons is the only source of initial modulation. First, we consider a sinusoidal density modulation along the x' coordinate at the entrance of the bunch compressor with period $\lambda_{x'} = \sqrt{2\pi}\sigma_{x'}/h$, where $\sigma_{x'}$ is the rms angular beam size, and h is the harmonic number. According to (9), this modulation emerges as the longitudinal density modulation in the telescope section with period $\lambda_z = \sqrt{2\pi}\sigma_s/h$, where $\sigma_s = |\eta|\sigma_{x'}$ is the rms bunch length in the telescope section for a case $\xi \equiv 0$ assumed here for simplicity. Using the model for a space charge induced longitudinal electric field described in [5, 6], and assuming that the density modulation is defined by Poisson statistics, we obtain for the energy modulation at the end of the telescope section:

$$\Delta\delta(h,z) = \frac{2 r_0 L}{\pi \gamma a^2} \sqrt{\frac{N}{h}} \left(1 - 2I_1(hx_0)K_1(hx_0)\right)\sin(\sqrt{2\pi}hz/\sigma_s), \qquad (13)$$

where N is the total number of particles in the bunch, r_0 is the classical radius of the particle, L is the length of the telescope section, $x_0 = \sqrt{2\pi}a/\gamma\sigma_s$, I_1 and K_1 are modified Bessel functions of

the first and second kind, and $a = 1.747(\sigma_{xT} + \sigma_{yT})/2$, where $\sigma_{xT} \approx \sqrt{\beta_T \varepsilon_z}$ is the average

horizontal beam size and $\sigma_{yT} \approx \sqrt{\beta_T \varepsilon_y}$ is the average vertical beam size in the telescope section

[6]. Here we use longitudinal emittance ε_z before the bunch compressor and average beta-

function β_T inside the telescope section to estimate σ_{xT}, and vertical emittance ε_y to estimate

σ_{yT}. Now, using (9), we find modulation in the horizontal coordinate after the second emittance

exchange at the end of the bunch compressor $\Delta x(h, x') = \eta \Delta \delta(h, x')$, where we substitute z/σ_s

in (13) by $x'/\sigma_{x'}$ based on transformations (9) and (11). Then starting from the emittance

definition $\varepsilon_x^2 = <x^2><x'^2> - <xx'>^2$, we obtain

$$2\Delta\varepsilon_x \varepsilon_{x0} \approx <\Delta x(h, x')^2> \sigma_{x'}^2 - <\Delta x(h, x')x'>^2, \tag{14}$$

where $\Delta\varepsilon_x$ is the emittance increase, $\varepsilon_{x0} = \varepsilon_{xN}/\gamma$, and the symbol $<>$ defines averaging over

particle density distribution in x'. Next, using (13) and assuming a Gaussian distribution in x',

we obtain after neglecting small non-essential terms:

$$\frac{\Delta\varepsilon_x(h)}{\varepsilon_{x0}} \approx \left(\frac{r_0 L \eta \sigma_{x'}}{\pi \gamma a^2 \varepsilon_{x0}}\right)^2 \frac{N}{h}(1 - 2I_1(hx_0)K_1(hx_0))^2. \tag{15}$$

Using $L = 10$ m, $\beta_T = 10$ m and bunch charge $eN = 250$ pC, we calculate $\Delta\varepsilon_x(h)/\varepsilon_{x0}$, and plot it
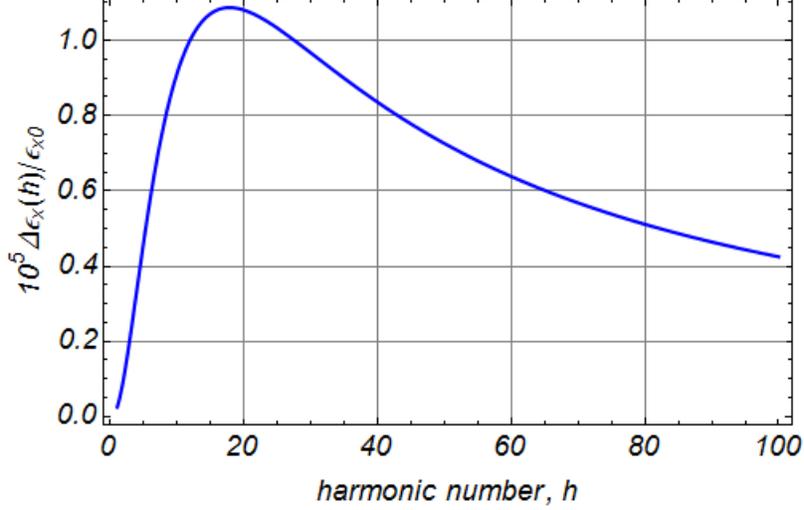
in Figure 3.

Figure 3. Relative emittance increase as a function of the harmonic number h of particle density modulation along the x′ coordinate at the entrance of the bunch compressor due to the shot noise of electrons.

As an estimate of the highest harmonic number we use the ratio of $\sqrt{2\pi}\sigma_s$ to the average distance between two electrons in the bunch, which we find in two steps: by defining the average distance between electrons in the co-moving frame and then by transforming it into the laboratory frame. In result we get:

$$h_{\max} \approx \gamma^{2/3} N^{1/3} (\eta\sigma_{x'})^{2/3} (\sigma_{xT}\sigma_{yT})^{-1/3} . \tag{16}$$

Finally, by summing the contributions of all harmonics up to $h_{\max}$, we find the total emittance increase of the order of 0.3%. This result may change after accounting for 3D effects at high harmonic numbers similar to [7].

Now we consider emittance degradation caused by synchrotron radiation inside the bending magnets of the emittance exchange sections. Evidently, this is only applicable to electron beams. Mostly we are concerned about coherent synchrotron radiation (CSR). We expect to have the strongest CSR in the bend magnets adjacent to the telescope section, where

12

the bunch length is the shortest, according to Figure 2. Assuming Gaussian distribution of the electron density, we estimate the electron energy loss/gain using Eq.(18) from [8]:

$$\Delta\delta(z) = -\frac{2}{3^{1/3}\sqrt{2\pi}} \frac{Nr_0 L_B}{\gamma R^{2/3}\sigma_s^{4/3}} F(z/\sigma_s) e^{-(\sigma_\theta \sigma_{xT}/\sigma_s)^2}, \tag{17}$$

where L_B and R are the bend magnet length and radius of the curvature, $\sigma_\theta \cong 0.8/\gamma \cdot (\sigma_s/\lambdabar_c)^{0.354}$ [9] is the rms value of the opening angle of the synchrotron radiation for a spectral component with reduced wavelength $\lambdabar = \sigma_s$, $\lambdabar_c = 2/3 \cdot (R/\gamma^3)$ is the reduced critical wavelength of the synchrotron radiation, and

$$F(z/\sigma_s) = \int_{-\infty}^{z/\sigma_s} \frac{dx'}{(x-x')^{4/3}} \frac{d}{dx'} e^{-x'^2/2}. \tag{18}$$

We note that Eq. (17) has an extra exponent comparing to the formula given in [8]. It accounts for reduction of the CSR intensity in the case of a beam with a large transverse size [10]. Starting with (17) and using (9), we obtain a perturbation in x after the second emittance exchange $\Delta x(x') = \eta\Delta\delta(h,x')$, where we also substitute z/σ_s with its equivalent $x'/\sigma_{x'}$. Now, using (14) we find a relative increase of the projected emittance:

$$\frac{\Delta\varepsilon_x}{\varepsilon_{x0}} \approx \left(\frac{1}{3^{1/3}\sqrt{\pi}} \frac{Nr_0 L_B}{\gamma R^{2/3}(\eta\sigma_{x'})^{1/3}\varepsilon_{x0}}\right)^2 (H_1 - H_2), \tag{19}$$

where $H_1 = <F(x'/\sigma_{x'})^2> \approx 0.60$ and $H_2 = (<(x'/\sigma_{x'})\cdot F(x'/\sigma_{x'})>)^2 \approx 0.036$, and where averaging has taken over the electron distribution in x' that is assumed to be Gaussian. Using a bend magnet with $L_B = 0.1$ m and $R = 1$ m, and keeping other parameters the same as above, we calculate less than 4% emittance increase. We note that the main reason the emittance increase is rather modest is due to a large beam transverse size inside the magnets that helps with suppression of the CSR; and the main reason the beam size is large is due to a relatively large

13

longitudinal emittance before the bunch compressor. Without that, the impact of the CSR will be much stronger. The electron density distribution in the horizontal phase space after the bunch compressor calculated using the above described beam parameters is shown in Figure 4.
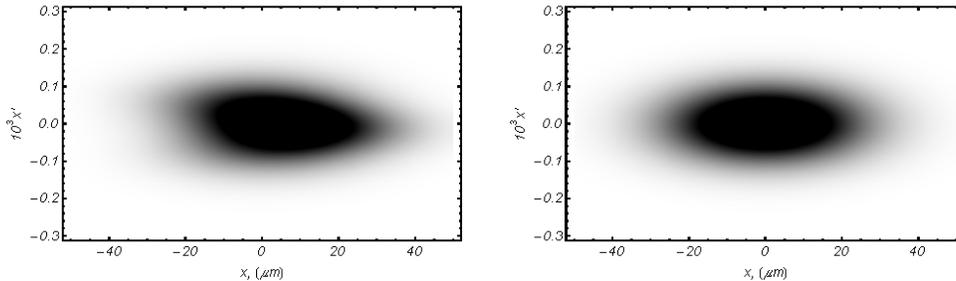

Figure 4. The electron density distribution in the horizontal phase space after the bunch compressor, with CSR taken into account (left side) and without the CSR (right side).

Ordinary incoherent synchrotron radiation is also able to affect electron beam emittance while the electron beam undergoes the chain of beam manipulations taking place during bunch compression. However, the impact of synchrotron radiation typically scales as $\gamma^{5/2}$ [11] and, thus, can be mitigated by an appropriate choice of electron beam energy.

4. Other applications

Here we discuss some possible applications that take advantage of the above described beam manipulations. First, we note that any time-dependent variation existing in the beam before bunch compressor will be compressed or expanded (if desired) after the bunch compressor, depending on the demagnification factor in the telescope. For example, one can produce time-dependent energy modulation of electrons using laser–electron beam interaction in the wiggler magnet upstream of the bunch compressor and either compress it or expand it with the bunch compressor. Because transformation (12) preserves the depth of the original modulation, the bunch compressor works as an ideal frequency converter. Moreover, the magnetic chicane at the end of the bunch compressor can also convert energy modulation into density modulation and

14

prepare the electron bunch for coherent radiation. Furthermore, the frequency of the radiation produced by this electron beam can be tuned using the telescope's demagnification factor.

Another option consists of modulating only a part of the electron bunch and compressing an entire electron bunch at relatively low electron beam energy, while deferring the microbunching to the high energy, after acceleration. Then the radiation produced by the part of the electron bunch with microbunching can be used as a seed signal for a free-electron laser (FEL) operating with the section of the electron bunch that remains "fresh" and without microbunching.

Yet another option is to use the microbunching obtained via the frequency down-conversion and generate THz radiation.

One more option consists of exploring a chirpless nature of a new compression scheme and adding a proposed bunch compressor into a chain of beam manipulations pioneered by a technique of echo-enabled harmonic generation (EEHG) [12]. The idea of merging the EEHG with the emittance exchange transformation was previously considered in [13], but our approach is fundamentally different. A proposal is to start with three EEHG steps and obtain a characteristic distribution of electrons in the longitudinal phase space shown in Figure 5a. Then, continue by sending the electron bunch through the above-described bunch compressor and squeezing its longitudinal size while expanding its energy dimension as shown in Figure 5b. All of these beam manipulations can be performed at relatively low beam energy. After that one can accelerate electrons, complete compression if needed, and obtain microbunching as shown in Figure 5c. Adding a bunch compressor to the chain of the beam manipulations helps to obtain microbunching at a much higher frequency than is possible using EEHG alone. Besides, bunching efficiency remains the same as if there was no bunch compressor. Thus, by following a

proposed scenario one can easily shorten the wavelength for seeding the FEL that is obtainable

using the EEHG technique by an order of a magnitude or better. In a numerical example shown

in Figure 5 we used a 200-nm wavelength laser and optimized three EEHG steps with the above-

described beam parameters to yield a maximum microbunching at the 20th harmonic of the laser

frequency. We also used the bunch compressor with $m = 10$. Then, after following all beam

manipulations described above using a simplified 1D code we obtained the final distribution of

electrons in the longitudinal phase space and calculated the bunching factor of 13% at a 1-nm

wavelength, i.e., a 200th harmonic of the laser frequency. This is the same bunching factor as

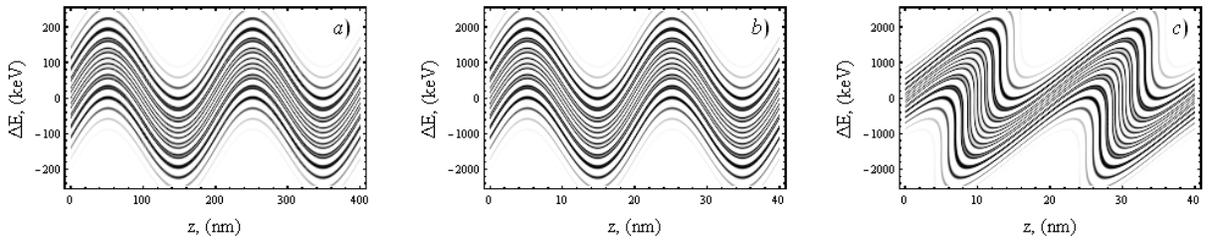EEHG alone will yield at a 20th harmonic.

Figure 5. The longitudinal phase space of the electron bunch : a) after the first three steps of the EEHG, b) after the bunch compressor, c) at the end of the acceleration and microbunching.

A different suite of applications can be served by beam shaping in the telescope section.

For example, a simple collimator installed there to cut beam tails in the transverse direction will

actually cut bunch tails in the longitudinal direction because of the downstream emittance

exchange transformation. Also a mask with a set of equally spaced vertical slits will produce a

train of equally spaced microbunches that can be used later to produce coherent radiation. A

proof-of-principle experiment for this idea was recently reported in [14]. The advantage of the

scheme with a double emittance exchange is the ability to obtain a train of microbunches with

better transverse emittance. Similarly, a mask with specially designed slits can create a train of

microbunches with a ramped peak current distribution and a "witness" bunch behind it which is often useful for the study of the wakefield acceleration in plasma and dielectric channel.

Adding a few-microns-thin beryllium foil into the telescope section easily increases energy spread after the bunch compressor due to multiple scattering of electrons in the foil. At the same time, added energy spread due to fluctuation of the energy losses in the foil is small, and no visible impact on the emittance after the bunch compressor is expected. In effect, this arrangement produces the same result as a "laser heater" [15] without the complexity of a laser heater.

This is only a small subset of beam manipulations in the longitudinal phase space afforded by the proposed double emittance exchange and beam manipulation in the transverse phase space in between.

5. Summary

In this paper we proposed a new type of bunch compressor based on two consecutive emittance exchange beam manipulations additionally equipped with a telescope between them. We followed this proposal with an extensive analysis and feasibility study. We also examined several collective effects and identified coherent synchrotron radiation as being potentially the most harmful. Then we demonstrated several other applications for the proposed bunch compressor including THz radiation and seeding of the FELs and short wavelength generation as well as shaping of the beam longitudinal density distribution in a way that is beneficial for several applications.

Appendix

The same result as given by Eq.(11) can be obtained by using for the emittance exchange lattice a four bend magnet chicane with a deflecting cavity in the middle of it. A transport matrix for the left and right leg of the chicane, i.e., from the beginning of the first magnet and to the end of the second magnet and from the beginning of the third magnet and to the end of the fourth magnet can be written:

$$
M_\pm = \begin{bmatrix} 1 & L & 0 & \pm\eta \\ 0 & 1 & 0 & 0 \\ 0 & \pm\eta & 1 & \xi \\ 0 & 0 & 0 & 1 \end{bmatrix} \quad , \tag{A.1}
$$

where the sign + is for the left part and the sign − is for the right part. Additionally, a special lattice is required from the end of the second magnet to the beginning of the deflecting cavity with the transport matrix:

$$
TL = \begin{bmatrix} -b & bL+d/2b & 0 & 0 \\ 0 & -1/b & 0 & 0 \\ 0 & 0 & 1 & 0 \\ 0 & 0 & 0 & 1 \end{bmatrix} \tag{A.2}
$$

and from the end of the deflecting cavity to the beginning of the third magnet with the transport matrix:

$$
TR = \begin{bmatrix} -1/b & bL+d/2b & 0 & 0 \\ 0 & -b & 0 & 0 \\ 0 & 0 & 1 & 0 \\ 0 & 0 & 0 & 1 \end{bmatrix} \tag{A.3}
$$

18

Together with the deflecting cavity described by the transport matrix of the Eq.(6), the entire arrangement gives for the emittance exchange lattice:

$$EEX = \begin{bmatrix} 0 & 0 & 0 & \eta \\ 0 & 0 & bk & bk\xi \\ bk\xi & \eta & 0 & 0 \\ bk & 0 & 0 & 0 \end{bmatrix} \qquad (A.4)$$

This is equivalent to Eq.(9) with the substitution $k \rightarrow bk$. We note that using $|b| > 1$ provides a boost of the dispersion function in the deflecting cavity increasing it from η to $\eta_1 = b\eta$ in an agreement with a proposal from [16]. Then a condition $k\eta_1 \equiv 1$ must be satisfied in order to yield Eq.(A.4).

References

[1] M. Cornacchia, P. Emma, Phys. Rev. Spec. Topics – Acc. and Beams, **5**, 084001 (2002).

[2] M. Dohlus, T. Limberg and P. Emma, 2005 Beam Dynamics Newsletter, http://www-bd.fnal.gov/icfabd/Newsletter38.pdf.

[3] P. Emma, Z. Huang, K.-J. Kim, P. Piot, Phys. Rev. Spec. Topics – Acc. and Beams, **9**, 100702 (2006).

[4] J. Ruan *et al*., http://arxiv.org/abs/1102.3155 , (January 15, 2011).

[5] J. Rosenzweig, C. Pellegrini, L. Serafini, C. Ternienden and G. Travish, Proceedings of the Advanced Accelerator Workshop, Lake Tahoe, October 12-18, 1996 (1996).

[6] J. Qiang, R. D. Ryne, M. Venturini, and A. Zholents, Phys. Rev. Spec. Topics – Acc. and Beams, **12**, 100702 (2009).

[7] M. Venturini, Phys. Rev. Spec. Topics – Acc. and Beams **11**, 034401 (2008).

[8] Ya. Derbenev, J. Rossbach, E. Saldin, and V. Shiltsev, TESLA-FEL 95-05 (1995).

[9] K.-J. Kim, X-ray data booklet, LBNL-PUB-490, Rev. 2, (2001).

[10] C. Neuman, W. Graves, P. O'Shea, Phys. Rev. Spec. Topics – Acc. and Beams, **3**, 030701 (2000).

[11] A.W. Chao and M. Tigner, *Handbook of Accelerator Physics and Engineering*, (World Scientific, Singapore, 2006).

[12] G. Stupakov, Phys. Rev. Lett. **102**, 074801, 1-4 (2009).

[13] B. Jiang, J. Power, R. Lindberg, W. Liu and W. Gai, Phys. Rev. Lett., **106**, 114901(2011).

[14] Y.-E. Sun *et al*., Phys. Rev. Lett. **105**, 234801 (2010).

[15] Z. Huang *et al*., Phys. Rev. Spec. Topics – Acc. and Beams, **13**, 020703 (2010).

[16] D. Xiang, A. Chao, Proc. Part. Acc. Conf., NY, WEB044, (2011).